arXiv:hep-ph/0204341v1 29 Apr 2002

BUTP–02/06
hep-ph/0204341

Complete gluon bremsstrahlung corrections to the process $b \to s\,\ell^+\ell^-$ *

H.H. Asatryan[a], H.M. Asatrian[a], C. Greub[b] and M. Walker[b]

[a] *Yerevan Physics Institute, 2 Alikhanyan Br., 375036 Yerevan, Armenia*
[b] *Institut für Theoretische Physik, Universität Bern, CH–3012 Bern, Switzerland.*

ABSTRACT

In a recent paper [1], we presented the calculation of the $\mathcal{O}(\alpha_s)$ virtual corrections to $b \to s\,\ell^+\ell^-$ and of those bremsstrahlung terms which are needed to cancel the infrared divergences. In the present paper we work out the remaining $\mathcal{O}(\alpha_s)$ bremsstrahlung corrections to $b \to s\,\ell^+\ell^-$, which do not suffer from infrared and collinear singularities. These new contributions turn out to be small numerically. In addition, we also investigate the impact of the definition of m_c on the numerical results.

---

*Work partially supported by Schweizerischer Nationalfonds and SCOPES program

1 Introduction

The inclusive rare decay $B \to X_s\, \ell^+\ell^-$ has not been observed so far, but is expected to be measured at the operating B factories after a few years of data taking. The measurement of its various kinematical distributions, combined with improved data on $B \to X_s\, \gamma$, will imply tight constraints on the extensions of the standard model and perhaps even reveal some new physics.

The main problem of the theoretical description of $B \to X_s\, \ell^+\ell^-$ is due to the long-distance contributions from $\bar{c}c$ resonant states. When the invariant mass $\sqrt{s}$ of the lepton pair is close to the mass of a resonance, only model dependent predictions for these long distance contributions are available today. It is therefore unclear whether the theoretical uncertainty can be reduced to less than ±20% when integrating over these domains [2].

However, when restricting $\sqrt{s}$ to a region below the resonances, the long distance effects are under control. The corrections to the pure perturbative picture can be analyzed within the heavy quark effective theory (HQET). In particular, all available studies indicate that for the region $0.05 < \hat{s} = s/m_b^2 < 0.25$ the non-perturbative effects are below 10% [3, 4, 5, 6, 7, 8]. Consequently, the differential decay rate for $B \to X_s\, \ell^+\ell^-$ can be precisely predicted in this region using renormalization group improved perturbation theory. It was pointed out in the literature that the differential decay rate and the forward-backward asymmetry are particularly sensitive to new physics in this kinematical window [9, 10, 11, 12, 13].

The next-to-leading logarithmic (NLL) result for $B \to X_s\, \ell^+\ell^-$ suffers from a relatively large (±16%) dependence on the matching scale μ_W [14, 15]. The NNLL corrections to the Wilson coefficients remove the matching scale dependence to a large extent [16], but leave a ±13%-dependence on the renormalization scale μ_b, which is of $\mathcal{O}(m_b)$. In order to further improve the theoretical prediction, we have recently calculated the $\mathcal{O}(\alpha_s)$ virtual two-loop corrections to the matrix elements $\langle s\, \ell^+\ell^- | O_i | b \rangle$ $(i = 1, 2)$ as well as the virtual $\mathcal{O}(\alpha_s)$ one-loop corrections to O_7,..., O_{10} [1]. As some of these corrections suffer from infrared and collinear singularities, we have added those bremsstrahlung corrections needed to cancel these singularities. This improvement reduced the renormalization scale dependence by a factor of 2.

In the present paper we complete the calculation of the bremsstrahlung corrections associated with the operators O_1, O_2, O_7,...,O_{10}, i.e., we add those bremsstrahlung terms which are purely finite and have therefore been omitted in Ref. [1]. We anticipate that the additional terms have a small impact on the phenomenology of $b \to s\, \ell^+\ell^-$.

The paper is organized as follows: In Sec. 2, we briefly specify the theoretical framework, before, in Sec. 3, we discuss the organization of the calculation of the finite bremsstrahlung corrections and review the structure of the virtual corrections and singular bremsstrahlung contributions, calculated in Ref. [1]. The finite bremsstrahlung corrections are worked out in Sec. 4 and Sec. 5. In Sec. 6, finally, we investigate the numerical impact of the new corrections on the invariant mass spectrum of the lepton pair. We also illustrate the dependence of our results on the definition of the charm quark mass.

2 Effective Hamiltonian

The appropriate tool for studies on weak B mesons decays is the effective Hamiltonian technique. The effective Hamiltonian is derived from the standard model by integrating out the t quark, the Z_0 and the W boson. For the decay channels $b \to s\,\ell^+\ell^-$ ($\ell = \mu, e$) it reads

$$\mathcal{H}_{\text{eff}} = -\frac{4\,G_F}{\sqrt{2}}\,V_{ts}^*\,V_{tb}\sum_{i=1}^{10} C_i\,O_i\,,$$

where O_i are dimension six operators and C_i denote the corresponding Wilson coefficients. The operators we choose as in [16]:

$$\begin{array}{rclrcl}
O_1 &=& (\bar{s}_L\gamma_\mu T^a c_L)(\bar{c}_L\gamma^\mu T^a b_L), & O_2 &=& (\bar{s}_L\gamma_\mu c_L)(\bar{c}_L\gamma^\mu b_L),\\
O_3 &=& (\bar{s}_L\gamma_\mu b_L)\sum_q(\bar{q}\gamma^\mu q), & O_4 &=& (\bar{s}_L\gamma_\mu T^a b_L)\sum_q(\bar{q}\gamma^\mu T^a q),\\
O_5 &=& (\bar{s}_L\gamma_\mu\gamma_\nu\gamma_\sigma b_L)\sum_q(\bar{q}\gamma^\mu\gamma^\nu\gamma^\sigma q), & O_6 &=& (\bar{s}_L\gamma_\mu\gamma_\nu\gamma_\sigma T^a b_L)\sum_q(\bar{q}\gamma^\mu\gamma^\nu\gamma^\sigma T^a q),\\
O_7 &=& \frac{e}{g_s^2}m_b(\bar{s}_L\sigma^{\mu\nu}b_R)F_{\mu\nu}, & O_8 &=& \frac{1}{g_s}m_b(\bar{s}_L\sigma^{\mu\nu}T^a b_R)G^a_{\mu\nu},\\
O_9 &=& \frac{e^2}{g_s^2}(\bar{s}_L\gamma_\mu b_L)\sum_\ell(\bar{\ell}\gamma^\mu\ell), & O_{10} &=& \frac{e^2}{g_s^2}(\bar{s}_L\gamma_\mu b_L)\sum_\ell(\bar{\ell}\gamma^\mu\gamma_5\ell).
\end{array}$$

The subscripts L and R refer to left- and right-handed fermion fields. We work in the approximation where the combination $(V_{us}^*V_{ub})$ of Cabibbo-Kobayashi-Maskawa (CKM) matrix elements is neglected and the CKM structure factorizes.

In the following it is convenient to define the operators $\widetilde{O}_7$,..., $\widetilde{O}_{10}$ according to

$$\widetilde{O}_j = \frac{\alpha_s}{4\,\pi}\,O_j\;, \quad (j = 7, ..., 10)\,, \tag{1}$$

with the corresponding coefficients

$$\widetilde{C}_j = \frac{4\,\pi}{\alpha_s}\,C_j\;, \quad (j = 7, ..., 10)\,. \tag{2}$$

3 Organization of the calculation and previous results

In this section we comment on the organization of the calculation of the virtual and bremsstrahlung corrections to the process $b \to s\,\ell^+\ell^-$ and repeat the results obtained in Ref. [1].

The one-loop diagrams in Fig. 1, associated with the four-quark operators O_1,..., O_6, lead to contributions which are proportional to the tree level matrix elements of the operators

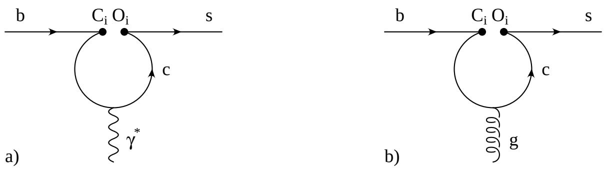

Figure 1: Diagram (a) can be absorbed by replacing the Wilson coefficients $\widetilde{C}_7$ and $\widetilde{C}_9$ through $\widetilde{C}_7^{\mathrm{mod}}$ and $\widetilde{C}_9^{\mathrm{mod}}$, respectively. γ^* denotes an off-shell photon which subsequently decays into a $(\ell^+\ell^-)$ pair. Similarly, diagram (b) is absorbed through the replacement $\widetilde{C}_8 \to \widetilde{C}_8^{\mathrm{mod}}$. g denotes an on-shell gluon. The index i runs from 1 to 6. See text for details.

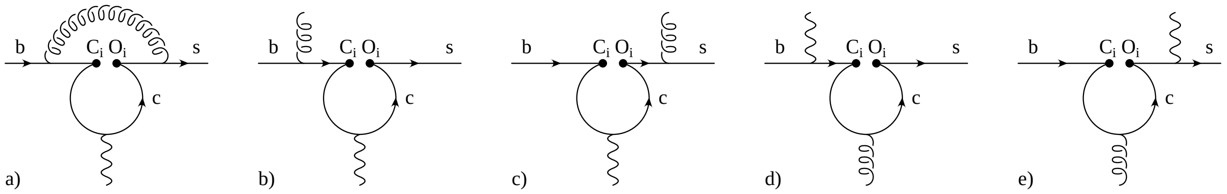

Figure 2: Diagrams which are automatically taken into account when calculating corrections to $\widetilde{C}_7^{(0,\mathrm{mod})}\widetilde{O}_7$, $\widetilde{C}_8^{(0,\mathrm{mod})}\widetilde{O}_8$ and $\widetilde{C}_9^{(0,\mathrm{mod})}\widetilde{O}_9$.

$\widetilde{O}_7$, $\widetilde{O}_8$ and $\widetilde{O}_9$. Therefore, they can be absorbed by appropriately modifying the Wilson coefficients $\widetilde{C}_7$, $\widetilde{C}_8$ and $\widetilde{C}_9$. The modified coefficients we write as

$$\begin{aligned}
\widetilde{C}_7^{\mathrm{mod}} &= A_7, \\
\widetilde{C}_8^{\mathrm{mod}} &= A_8, \\
\widetilde{C}_9^{\mathrm{mod}} &= A_9 + T_9\, h(z,\hat{s}) + U_9\, h(1,\hat{s}) + W_9\, h(0,\hat{s})\,.
\end{aligned} \tag{3}$$

The auxiliary quantities A_i, T_9, U_9 and W_9 are linear combinations of the Wilson coefficients $C_i(\mu)$. Their explicit form is relegated to the appendix. The one-loop function $h(z,\hat{s})$ is given by [16]

$$\begin{aligned}
h(z,\hat{s}) = {} & -\frac{4}{9}\ln(z) + \frac{8}{27} + \frac{16}{9}\frac{z}{\hat{s}} \\
& - \frac{2}{9}\left(2 + \frac{4\,z}{\hat{s}}\right)\sqrt{\left|\frac{4\,z-\hat{s}}{\hat{s}}\right|}\cdot
\begin{cases}
2\arctan\sqrt{\frac{\hat{s}}{4\,z-\hat{s}}}\;, & \hat{s} < 4\,z \\
\ln\left(\frac{\sqrt{\hat{s}}+\sqrt{\hat{s}-4\,z}}{\sqrt{\hat{s}}-\sqrt{\hat{s}-4\,z}}\right) - i\,\pi, & \hat{s} > 4\,z
\end{cases}\,.
\end{aligned} \tag{4}$$

It is obvious that the modification of the Wilson coefficients automatically accounts also for the diagrams in Fig. 2 when calculating the corresponding corrections to the matrix elements

$$\langle s\,\ell^+\ell^-|\widetilde{C}_i^{(0,\mathrm{mod})}\widetilde{O}_i|b\rangle \quad (i=7,8,9),$$

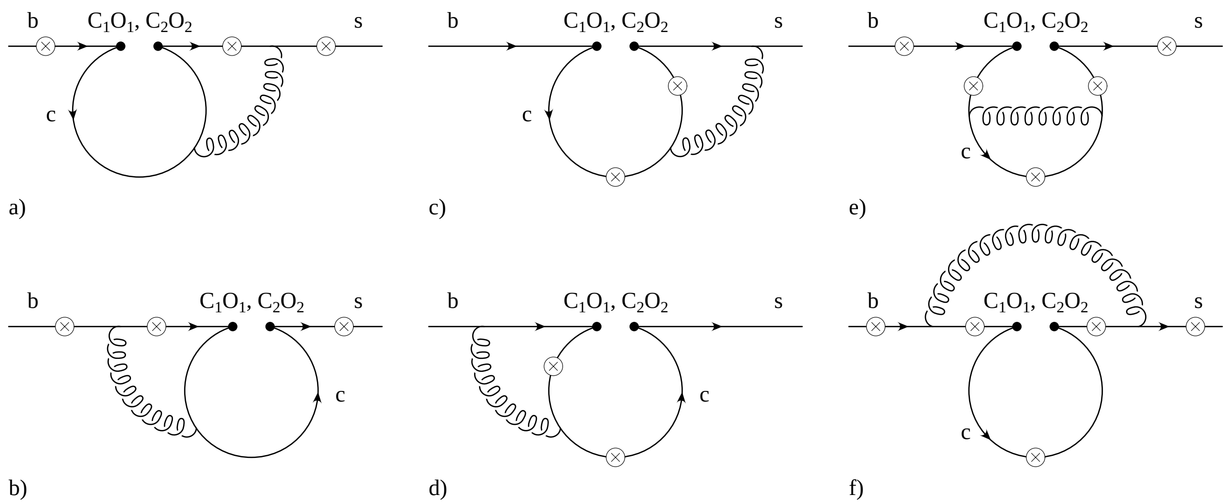

Figure 3: The two-loop virtual diagrams induced by O_1 and O_2 that cannot be absorbed into the $\widetilde{O}_{7,8,9}$ contributions by weighing them with the modified Wilson coefficients. The circle-crosses denote the possible locations where the virtual photon is emitted. The curly lines represent gluons.

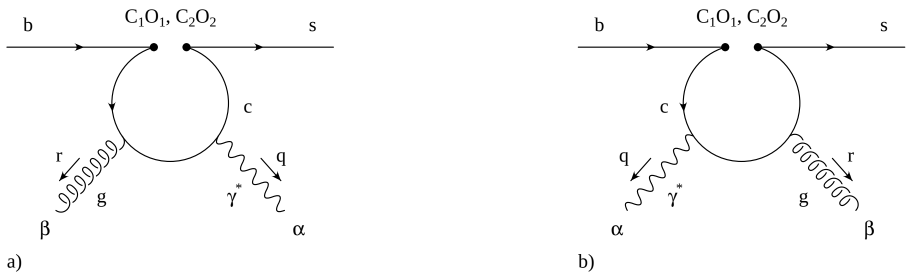

Figure 4: The only two bremsstrahlung diagrams induced by O_1 and O_2 that cannot be absorbed into the $\widetilde{O}_{7,8,9}$ contributions by weighing them with the modified Wilson coefficients.

where $\widetilde{C}_i^{(0,\mathrm{mod})}$ are the leading order terms of the modified Wilson coefficients, i.e.,

$$\begin{aligned}
\widetilde{C}_7^{(0,\mathrm{mod})} &= A_7^{(0)}, \\
\widetilde{C}_8^{(0,\mathrm{mod})} &= A_8^{(0)}, \\
\widetilde{C}_9^{(0,\mathrm{mod})} &= A_9^{(0)} + T_9^{(0)}\, h(z,\hat{s}) + U_9^{(0)}\, h(1,\hat{s}) + W_9^{(0)}\, h(0,\hat{s})\,.
\end{aligned} \tag{5}$$

For the explicit expressions of the quantities $A_i^{(0)}$, $T_9^{(0)}$, $U_9^{(0)}$ and $W_9^{(0)}$ we refer to the appendix.

Notice that the virtual and bremsstrahlung corrections of the four-quark operators with topologies shown in Figs. 3 and 4, however, have to be calculated explicitly. As the Wilson

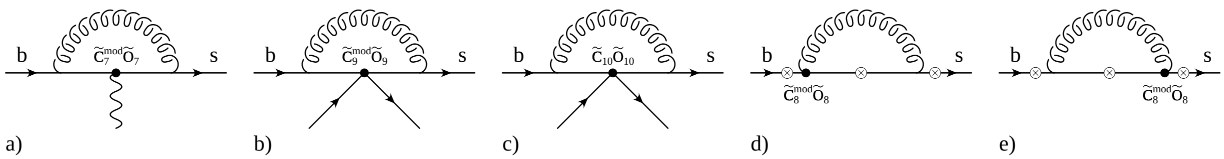
b
$\widetilde{C}_7^{\rm mod}\widetilde{O}_7$
s
a)
b
$\widetilde{C}_9^{\rm mod}\widetilde{O}_9$
s
b)
b
$\widetilde{C}_{10}\widetilde{O}_{10}$
s
c)
b
s
$\widetilde{C}_8^{\rm mod}\widetilde{O}_8$
d)
b
s
$\widetilde{C}_8^{\rm mod}\widetilde{O}_8$
e)

Figure 5: One-loop virtual $\mathcal{O}(\alpha_s)$ corrections induced by $\widetilde{C}_7^{(0,\text{mod})}\widetilde{O}_7$, $\widetilde{C}_8^{(0,\text{mod})}\widetilde{O}_8$, $\widetilde{C}_9^{(0,\text{mod})}\widetilde{O}_9$ and $\widetilde{C}_{10}^{(0)}\widetilde{O}_{10}$. The circle-crosses denote the possible locations for emission of a virtual photon.

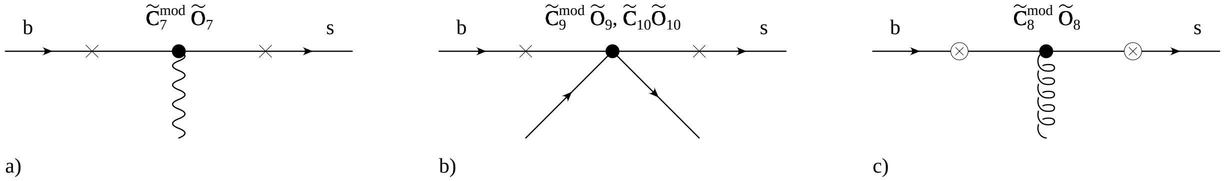
$\widetilde{C}_7^{\rm mod}\,\widetilde{O}_7$
b
s
a)
$\widetilde{C}_9^{\rm mod}\,\widetilde{O}_9, \widetilde{C}_{10}\widetilde{O}_{10}$
b
s
b)
$\widetilde{C}_8^{\rm mod}\,\widetilde{O}_8$
b
s
c)

Figure 6: The $\mathcal{O}(\alpha_s)$ bremsstrahlung diagrams induced by $\widetilde{O}_7$, $\widetilde{O}_9$, $\widetilde{O}_{10}$ and $\widetilde{O}_8$. Weighing the contributions of $\widetilde{O}_7$, $\widetilde{O}_8$ and $\widetilde{O}_9$ with the corresponding modified Wilson coefficients accounts for the bremsstrahlung diagrams depicted in Fig. 2 (b)–(e). The crosses and circle-crosses denote the possible locations for emission of a bremsstrahlung gluon and a virtual photon, respectively.

coefficients C_1 and C_2 are much larger than C_3,...,C_6 we retain the contributions of these topologies only for O_1 and O_2 insertions.

In the previous work [1], we systematically calculated the virtual corrections to the matrix elements of $C_1^{(0)}O_1$, $C_2^{(0)}O_2$, shown in Fig. 3, as well as to those of $\widetilde{C}_j^{(0,\text{mod})}\widetilde{O}_j$ $(j = 7, ..., 9)$ and $\widetilde{C}_{10}^{(0)}\widetilde{O}_{10}$ (cf Fig. 5). Furthermore, we also took into account the corrections to the Wilson coefficients calculated in Refs. [16, 17].

We found that the matrix elements of the operators $\widetilde{O}_7$, $\widetilde{O}_9$ and $\widetilde{O}_{10}$ [cf Fig. 5(a)–(c)] suffer from infrared and collinear singularities. Consequently, on decay width level the interferences $(\widetilde{O}_j, \widetilde{O}_k)$ $(j, k = 7, 9, 10)$ are singular, too. We therefore included the gluon bremsstrahlung corrections associated with $(\widetilde{O}_j, \widetilde{O}_k)$ $(j, k = 7, 9, 10)$ in order to get an infrared finite result for the decay width [cf Fig. 6(a) and (b)].

Taking into account the virtual and bremsstrahlung contributions discussed so far, we obtain the result presented in Ref. [1]:

$$\frac{d\Gamma(b \to X_s\,\ell^+\ell^-)}{d\hat{s}} = \left(\frac{\alpha_{em}}{4\,\pi}\right)^2 \frac{G_F^2\, m_{b,\text{pole}}^5\, \left|V_{ts}^* V_{tb}\right|^2}{48\,\pi^3} (1-\hat{s})^2 \times \left\{ (1+2\,\hat{s}) \left(\left|\widetilde{C}_9^{\text{eff}}\right|^2 + \left|\widetilde{C}_{10}^{\text{eff}}\right|^2 \right) + 4\,(1+2/\hat{s}) \left|\widetilde{C}_7^{\text{eff}}\right|^2 + 12\,\text{Re}\left(\widetilde{C}_7^{\text{eff}} \widetilde{C}_9^{\text{eff}*}\right) \right\}, \quad (6)$$

where the effective Wilson coefficients $\widetilde{C}_7^{\rm eff}$, $\widetilde{C}_9^{\rm eff}$ and $\widetilde{C}_{10}^{\rm eff}$ are given by [1]

$$\begin{aligned}\widetilde{C}_7^{\rm eff} &= \left(1+\frac{\alpha_s(\mu)}{\pi}\,\omega_7(\hat{s})\right)\,A_7\\ &\quad -\frac{\alpha_s(\mu)}{4\,\pi}\left(C_1^{(0)}F_1^{(7)}(\hat{s})+C_2^{(0)}F_2^{(7)}(\hat{s})+A_8^{(0)}F_8^{(7)}(\hat{s})\right), \end{aligned} \tag{7}$$

$$\begin{aligned}\widetilde{C}_9^{\rm eff} &= \left(1+\frac{\alpha_s(\mu)}{\pi}\,\omega_9(\hat{s})\right)\left(A_9+T_9\,h(\hat{m}_c^2,\hat{s})+U_9\,h(1,\hat{s})+W_9\,h(0,\hat{s})\right)\\ &\quad -\frac{\alpha_s(\mu)}{4\,\pi}\left(C_1^{(0)}F_1^{(9)}(\hat{s})+C_2^{(0)}F_2^{(9)}(\hat{s})+A_8^{(0)}F_8^{(9)}(\hat{s})\right), \end{aligned} \tag{8}$$

$$\widetilde{C}_{10}^{\rm eff} = \left(1+\frac{\alpha_s(\mu)}{\pi}\,\omega_9(\hat{s})\right)\,A_{10}. \tag{9}$$

The quantities $C_1^{(0)}$, $C_2^{(0)}$, A_7, $A_8^{(0)}$, A_9, A_{10}, T_9, U_9 and W_9 are Wilson coefficients or linear combinations thereof. We give their analytical expressions and numerical values in the appendix. The one-loop function $h(\hat{m}_c^2,\hat{s})$ is given in Eq. (4), while the two-loop functions $F_{1,2}^{(7),(9)}$, accounting for the diagrams in Fig. 3, and the one-loop functions $F_8^{(7),(9)}$, corresponding to the diagrams 5(d) and (e), are given in Ref. [1]. The functions ω_7 and ω_9, finally, include both virtual and bremsstrahlung corrections associated with $\widetilde{O}_7$, $\widetilde{O}_9$ and $\widetilde{O}_{10}$. For details on their construction we again refer to [1].

When calculating the decay width (6), we retain only terms linear in α_s (and thus in ω_7, ω_9) in the expressions for $|\widetilde{C}_7^{\rm eff}|^2$, $|\widetilde{C}_9^{\rm eff}|^2$ and $|\widetilde{C}_{10}^{\rm eff}|^2$. In the interference term $\mathrm{Re}\left(\widetilde{C}_7^{\rm eff}\widetilde{C}_9^{\rm eff*}\right)$ too, we keep only linear contributions in α_s. By construction one has to make the replacements $\omega_9 \to \omega_{79}$ and $\omega_7 \to \omega_{79}$ in this term.

The functions ω_7, ω_9 and ω_{79} read

$$\begin{aligned}\omega_7(\hat{s}) &= -\frac{8}{3}\,\ln\left(\frac{\mu}{m_b}\right)-\frac{4}{3}\,\mathrm{Li}(\hat{s})-\frac{2}{9}\,\pi^2-\frac{2}{3}\,\ln(\hat{s})\ln(1-\hat{s})\\ &\quad -\frac{1}{3}\,\frac{8+\hat{s}}{2+\hat{s}}\ln(1-\hat{s})-\frac{2}{3}\,\frac{\hat{s}\,(2-2\,\hat{s}-\hat{s}^2)}{(1-\hat{s})^2\,(2+\hat{s})}\ln(\hat{s})-\frac{1}{18}\,\frac{16-11\,\hat{s}-17\,\hat{s}^2}{(2+\hat{s})\,(1-\hat{s})}\,, \end{aligned} \tag{10}$$

$$\begin{aligned}\omega_9(\hat{s}) &= -\frac{4}{3}\,\mathrm{Li}(\hat{s})-\frac{2}{3}\ln(1-\hat{s})\ln(\hat{s})-\frac{2}{9}\pi^2-\frac{5+4\,\hat{s}}{3(1+2\,\hat{s})}\ln(1-\hat{s})\\ &\quad -\frac{2\,\hat{s}\,(1+\hat{s})(1-2\,\hat{s})}{3\,(1-\hat{s})^2(1+2\,\hat{s})}\ln(\hat{s})+\frac{5+9\,\hat{s}-6\,\hat{s}^2}{6\,(1-\hat{s})(1+2\,\hat{s})}\,, \end{aligned} \tag{11}$$

$$\omega_{79}(\hat{s}) = -\frac{4}{3}\ln\left(\frac{\mu}{m_b}\right) - \frac{4}{3}\,\mathrm{Li}(\hat{s}) - \frac{2}{9}\,\pi^2 - \frac{2}{3}\ln(\hat{s})\ln(1-\hat{s}) - \frac{1}{9}\,\frac{2+7\,\hat{s}}{\hat{s}}\ln(1-\hat{s}) - \frac{2}{9}\,\frac{\hat{s}\,(3-2\,\hat{s})}{(1-\hat{s})^2}\ln(\hat{s}) + \frac{1}{18}\,\frac{5-9\,\hat{s}}{1-\hat{s}}\,. \quad (12)$$

Summary

The bremsstrahlung corrections associated with the interferences

$$\left(\widetilde{C}_j^{(0,\mathrm{mod})}\widetilde{O}_j, \widetilde{C}_k^{(0,\mathrm{mod})}\widetilde{O}_k\right), \quad (j,k=7,9,10),$$

are already included in formula (6). The remaining bremsstrahlung corrections, which are infrared finite, we derive in Sec. 4 and Sec. 5. In Sec. 4 we discuss the contributions of the interferences

$$\left(\widetilde{C}_8^{(0,\mathrm{mod})}\widetilde{O}_8, \widetilde{C}_k^{(0,\mathrm{mod})}\widetilde{O}_k\right), \quad (k=7,8,9,10)\,,$$

which we call to be of type A. There is no contribution from $k=10$ because of the Dirac structures of the involved operators. Sec. 5 is devoted to the interferences

$$\left(C_i^{(0)}O_i, C_j^{(0)}O_j\right), \ (i,j=1,2) \quad \text{and} \quad \left(C_i^{(0)}O_i, \widetilde{C}_k^{(0,\mathrm{mod})}\widetilde{O}_k\right), \ (i=1,2;\ k=7,8,9,10)\,.$$

Accordingly, we call these the type B terms. Again, the contributions for $k=10$ vanish due to the Dirac structures of the operators involved.

4 Finite bremsstrahlung contributions of type A

The bremsstrahlung contributions taken into account by introducing the functions $\omega_i(\hat{s})$ cancel the infrared divergences associated with the virtual corrections. All other bremsstrahlung terms are finite. This allows us to perform their calculation directly in $d=4$ dimensions.

The bremsstrahlung contributions from $\widetilde{O}_7-\widetilde{O}_8$ and $\widetilde{O}_8-\widetilde{O}_9$ interference terms as well as the $\widetilde{O}_8-\widetilde{O}_8$ term oppose no difficulties. The sum of these three parts can be written as

$$\frac{d\Gamma^{\mathrm{Brems,A}}}{d\hat{s}} = \frac{d\Gamma^{\mathrm{Brems}}_{78}}{d\hat{s}} + \frac{d\Gamma^{\mathrm{Brems}}_{89}}{d\hat{s}} + \frac{d\Gamma^{\mathrm{Brems}}_{88}}{d\hat{s}} = \left(\frac{\alpha_{em}}{4\,\pi}\right)^2\left(\frac{\alpha_s}{4\,\pi}\right)\frac{m^5_{b,\mathrm{pole}}\,|V^*_{ts}\,V_{tb}|^2\,G_F^2}{48\,\pi^3} \times \Big(2\,\mathrm{Re}\big[c_{78}\,\tau_{78}+c_{89}\,\tau_{89}\big]+c_{88}\,\tau_{88}\Big). \quad (13)$$

The coefficients c_{ij} are given by

$$c_{78} = C_F\cdot\widetilde{C}_7^{(0,\mathrm{eff})}\widetilde{C}_8^{(0,\mathrm{eff})*}, \quad c_{89} = C_F\cdot\widetilde{C}_8^{(0,\mathrm{eff})}\widetilde{C}_9^{(0,\mathrm{eff})*}, \quad c_{88} = C_F\cdot\left|\widetilde{C}_8^{(0,\mathrm{eff})}\right|^2, \quad (14)$$

while the quantities τ_{ij} read

$$
\begin{aligned}
\tau_{78} = \frac{8}{9\,\hat{s}} \Bigg\{ & 25 - 2\,\pi^2 - 27\,\hat{s} + 3\,\hat{s}^2 - \hat{s}^3 + 12\left(\hat{s} + \hat{s}^2\right)\,\ln(\hat{s}) \\
& + 6\left(\frac{\pi}{2} - \arctan\left[\frac{2 - 4\,\hat{s} + \hat{s}^2}{(2-\hat{s})\sqrt{\hat{s}}\,\sqrt{4-\hat{s}}}\right]\right)^2 - 24\,\mathrm{Re}\left(\mathrm{Li}\left[\frac{\hat{s} - i\sqrt{\hat{s}}\,\sqrt{4-\hat{s}}}{2}\right]\right) - \\
& 12\left((1-\hat{s})\sqrt{\hat{s}}\,\sqrt{4-\hat{s}} - 2\arctan\left[\frac{\sqrt{\hat{s}}\,\sqrt{4-\hat{s}}}{2-\hat{s}}\right]\right) \times \\
& \left(\arctan\left[\sqrt{\frac{4-\hat{s}}{\hat{s}}}\right] - \arctan\left[\frac{\sqrt{\hat{s}}\,\sqrt{4-\hat{s}}}{2-\hat{s}}\right]\right)\Bigg\},
\end{aligned}
\qquad (15)
$$

$$
\begin{aligned}
\tau_{88} = \frac{4}{27\,\hat{s}} \Bigg\{ & - 8\,\pi^2 + (1-\hat{s})\left(77 - \hat{s} - 4\,\hat{s}^2\right) - 24\,\mathrm{Li}(1-\hat{s}) \\
& + 3\left(10 - 4\,\hat{s} - 9\,\hat{s}^2 + 8\ln\left[\frac{\sqrt{\hat{s}}}{1-\hat{s}}\right]\right)\ln(\hat{s}) + 48\,\mathrm{Re}\left(\mathrm{Li}\left[\frac{3-\hat{s}}{2} + i\,\frac{(1-\hat{s})\sqrt{4-\hat{s}}}{2\sqrt{\hat{s}}}\right]\right) \\
& - 6\left(\frac{20\,\hat{s} + 10\,\hat{s}^2 - 3\,\hat{s}^3}{\sqrt{\hat{s}}\,\sqrt{4-\hat{s}}} - 8\,\pi + 8\arctan\left[\sqrt{\frac{4-\hat{s}}{\hat{s}}}\right]\right) \times \\
& \left(\arctan\left[\sqrt{\frac{4-\hat{s}}{\hat{s}}}\right] - \arctan\left[\frac{\sqrt{\hat{s}}\,\sqrt{4-\hat{s}}}{2-\hat{s}}\right]\right)\Bigg\},
\end{aligned}
\qquad (16)
$$

$$
\begin{aligned}
\tau_{89} = \frac{2}{3} \Bigg\{ & \hat{s}\,(4-\hat{s}) - 3 - 4\,\ln(\hat{s})\left(1 - \hat{s} - \hat{s}^2\right) \\
& - 8\,\mathrm{Re}\left(\mathrm{Li}\left[\frac{\hat{s}}{2} + i\,\frac{\sqrt{\hat{s}}\,\sqrt{4-\hat{s}}}{2}\right] - \mathrm{Li}\left[\frac{-2 + \hat{s}(4-\hat{s})}{2} + i\,\frac{(2-\hat{s})\sqrt{\hat{s}}\,\sqrt{4-\hat{s}}}{2}\right]\right) \\
& + 4\left(\hat{s}^2\sqrt{\frac{4-\hat{s}}{\hat{s}}} + 2\,\arctan\left[\frac{\sqrt{\hat{s}}\,\sqrt{4-\hat{s}}}{2-\hat{s}}\right]\right) \times \\
& \left(\arctan\left[\sqrt{\frac{4-\hat{s}}{\hat{s}}}\right] - \arctan\left[\frac{\sqrt{\hat{s}}\,\sqrt{4-\hat{s}}}{2-\hat{s}}\right]\right)\Bigg\}.
\end{aligned}
\qquad (17)
$$

5 Finite bremsstrahlung contributions of type B

In this section we consider the bremsstrahlung contributions from O_1 and O_2 and interference terms with $\widetilde{O}_7$, $\widetilde{O}_8$, $\widetilde{O}_9$ and $\widetilde{O}_{10}$. As mentioned before, interferences with $\widetilde{O}_{10}$ vanish due to the Dirac structures of the operators.

The bremsstrahlung contributions discussed in this section all involve the matrix elements associated with the two diagrams depicted in Fig. 4. Their sum, $\bar{J}_{\alpha\beta}$, is given by

$$\bar{J}_{\alpha\beta} = \frac{e\, g_s\, Q_u}{16\,\pi^2} \left[E(\alpha,\beta,r)\,\bar{\Delta}i_5 + E(\alpha,\beta,q)\,\bar{\Delta}i_6 - E(\beta,r,q)\frac{r_\alpha}{q\cdot r}\,\bar{\Delta}i_{23} \right.$$
$$\left. -E(\alpha,r,q)\frac{q_\beta}{q\cdot r}\,\bar{\Delta}i_{26} - E(\beta,r,q)\frac{q_\alpha}{q\cdot r}\,\bar{\Delta}i_{27} \right] L\,\frac{\lambda}{2}\,, \tag{18}$$

where q and r denote the momenta of the virtual photon and of the gluon, respectively. The index α will be contracted with the photon propagator, whereas β is contracted with the polarization vector $\epsilon^\beta(r)$ of the gluon. $\bar{J}_{\alpha\beta}$ and $\bar{\Delta}i_k$ are obtained from $J_{\alpha\beta}$ and Δi_k [1], respectively, by setting $r^2 = 0$ and dropping terms proportional to r_β. The matrix $E(\alpha,\beta,r)$ is defined as

$$E(\alpha,\beta,r) = \frac{1}{2}(\gamma_\alpha\gamma_\beta\not{r} - \not{r}\gamma_\beta\gamma_\alpha). \tag{19}$$

Due to Ward identities, the quantities $\bar{\Delta}i_k$ are not independent of one another. Namely,

$$q^\alpha \bar{J}_{\alpha\beta} = 0 \quad \text{and} \quad r^\beta \bar{J}_{\alpha\beta} = 0$$

imply that $\bar{\Delta}i_5$ and $\bar{\Delta}i_6$ can be expressed as

$$\bar{\Delta}i_5 = \bar{\Delta}i_{23} + \frac{q^2}{q\cdot r}\bar{\Delta}i_{27}\,; \quad \bar{\Delta}i_6 = \bar{\Delta}i_{26}\,. \tag{20}$$

As in addition $\bar{\Delta}i_{26} = -\bar{\Delta}i_{23}$, the bremsstrahlung matrix elements depend on $\bar{\Delta}i_{23}$ and $\bar{\Delta}i_{27}$, only. In $d = 4$ dimensions we find

$$\begin{aligned} \bar{\Delta}i_{23} &= 8\,(q\cdot r)\int_0^1 dx\,dy\,\frac{x\,y(1-y)^2}{C}\,, \\ \bar{\Delta}i_{27} &= 8\,(q\cdot r)\int_0^1 dx\,dy\,\frac{y\,(1-y)^2}{C}\,, \end{aligned} \tag{21}$$

where

$$C = m_c^2 - 2\,x\,y(1-y)(q\cdot r) - q^2\,y\,(1-y) - i\,\delta.$$

In the rest frame of the b quark and for fixed $\hat{s} = q^2/m_b^2$, the phase space integrals which one encounters in the calculation of $d\Gamma^{\text{Brems,B}}/d\hat{s}$ can be reduced to a two-dimensional integral over $\hat{E}_r = E_r/m_b$ and $\hat{E}_s = E_s/m_b$, where E_r and E_s are the energy of the gluon and the s quark, respectively. In the following it is useful to introduce the integration variable $w = 1 - 2\hat{E}_s$ instead of $\hat{E}_s$. The integration limits are then given by

$$\hat{E}_r \in \left[\frac{w-\hat{s}}{2}, \frac{w-\hat{s}}{2\,w}\right] \quad \text{and} \quad w \in [\hat{s}, 1].$$

For fixed values of $\hat{s}$, the quantities $\bar{\Delta} i_{23}$ and $\bar{\Delta} i_{27}$ depend only on the scalar product $q\cdot r$, which, in the rest frame of the b quark, is given by $(w-\hat{s})\, m_b^2/2$. The integration over $\hat{E}_r$ turns out to be of rational kind and can be performed analytically. The remaining integration over w, however, is more complicated and is done numerically. The result can be written as

$$\begin{aligned}\frac{d\Gamma^{\text{Brems,B}}}{d\hat{s}} &= \left(\frac{\alpha_{\text{em}}}{4\,\pi}\right)^2 \left(\frac{\alpha_s}{4\,\pi}\right) \frac{G_F^2\, m_{b,\text{pole}}^5\, |V_{ts}^*\, V_{tb}|^2}{48\,\pi^3} \times \\ \int\limits_{\hat{s}}^{1} dw &\left[(c_{11}+c_{12}+c_{22})\,\tau_{22} + 2\,\text{Re}\Big[(c_{17}+c_{27})\,\tau_{27} + (c_{18}+c_{28})\,\tau_{28} + (c_{19}+c_{29})\,\tau_{29}\Big]\right]. \quad (22)\end{aligned}$$

The quantities τ_{ij}, expressed in terms of $\bar{\Delta} i_{23}$ and $\bar{\Delta} i_{27}$, read

$$\begin{aligned}\tau_{22} &= \frac{8}{27}\frac{(w-\hat{s})(1-w)^2}{\hat{s}\,w^3} \times \left\{ \Big[3\,w^2 + 2\,\hat{s}^2(2+w) - \hat{s}\,w\,(5-2\,w)\Big]\, \left|\bar{\Delta} i_{23}\right|^2 + \right. \\ &\left. \Big[2\,\hat{s}^2\,(2+\,w) + \hat{s}\,w\,(1+2\,w)\Big]\, \left|\bar{\Delta} i_{27}\right|^2 + 4\,\hat{s}\Big[w\,(1-w) - \hat{s}\,(2+w)\Big] \cdot \text{Re}\left[\bar{\Delta} i_{23} \bar{\Delta} i_{27}^*\right] \right\} \quad (23)\end{aligned}$$

$$\begin{aligned}\tau_{27} = \frac{8}{3}\frac{1}{\hat{s}\,w} \times &\left\{ \Big[(1-w)\left(4\,\hat{s}^2 - \hat{s}\,w + w^2\right) + \hat{s}\,w\,(4+\hat{s}-w)\ln(w)\Big]\bar{\Delta} i_{23} \right. \\ &\left. - \Big[4\,\hat{s}^2\,(1-w) + \hat{s}\,w\,(4+\hat{s}-w)\,\ln(w)\Big]\bar{\Delta} i_{27} \right\} \quad (24)\end{aligned}$$

$$\begin{aligned}\tau_{28} &= \frac{8}{9}\frac{1}{\hat{s}\,w\,(w-\hat{s})} \times \left\{ \Big[(w-s)^2(2\,\hat{s}-w)(1-w)\Big]\bar{\Delta} i_{23} - \Big[2\,\hat{s}\,(w-\hat{s})^2(1-w)\Big]\bar{\Delta} i_{27} \right. \\ &\left. + \hat{s}\,w\Big[(1+2\,\hat{s}-2\,w)\bar{\Delta} i_{23} - 2\,(1+\hat{s}-w)\bar{\Delta} i_{27}\Big] \cdot \ln\left[\frac{\hat{s}}{(1+\hat{s}-w)(w^2+\hat{s}\,(1-w))}\right] \right\} \quad (25)\end{aligned}$$

$$\begin{aligned}\tau_{29} = \frac{4}{3}\frac{1}{w} \times &\left\{ \Big[2\,\hat{s}(1-w)(\hat{s}+w) + 4\,\hat{s}\,w\ln(w)\Big]\bar{\Delta} i_{23} - \right. \\ &\left. \Big[2\,\hat{s}(1-w)(\hat{s}+w) + w(3\,\hat{s}+w)\ln(w)\Big]\bar{\Delta} i_{27} \right\} \quad (26)\end{aligned}$$

The coefficients c_{ij} in Eq. (22) include the dependence on the Wilson coefficients and the color factors. Explicitly, they read

$$\begin{aligned}
c_{11} &= C_{\tau_1} \cdot \left|C_1^{(0)}\right|^2 , & c_{17} &= C_{\tau_2} \cdot C_1^{(0)} \widetilde{C}_7^{(0,\text{eff})*}, & c_{27} &= C_F \cdot C_2^{(0)} \widetilde{C}_7^{(0,\text{eff})*}, \\
c_{12} &= C_{\tau_2} \cdot 2\,\text{Re}\Big[C_1^{(0)} C_2^{(0)*}\Big] , & c_{18} &= C_{\tau_2} \cdot C_1^{(0)} \widetilde{C}_8^{(0,\text{eff})*}, & c_{28} &= C_F \cdot C_2^{(0)} \widetilde{C}_8^{(0,\text{eff})*}, \\
c_{22} &= C_F \cdot \left|C_2^{(0)}\right|^2 , & c_{19} &= C_{\tau_2} \cdot C_1^{(0)} \widetilde{C}_9^{(0,\text{eff})*}, & c_{29} &= C_F \cdot C_2^{(0)} \widetilde{C}_9^{(0,\text{eff})*},
\end{aligned} \tag{27}$$

where the color factors C_F, C_{τ_1} and C_{τ_2} arise from the following color structures:

$$\sum_a T^a T^a = C_F \mathbf{1}, \quad C_F = \frac{N_c^2-1}{2\,N_c} \,,$$

$$\sum_{a,b,c} T^a T^c T^a T^b T^c T^b = C_{\tau_1} \mathbf{1}, \quad C_{\tau_1} = \frac{N_c^2-1}{8\,N_c^3} \,,$$

and

$$\sum_{a,b} T^a T^b T^a T^b = C_{\tau_2} \mathbf{1}, \quad C_{\tau_2} = -\frac{N_c^2-1}{4\,N_c^2} \,.$$

Finally, we list the explicit formulas for $\bar{\Delta} i_{23}$ and $\bar{\Delta} i_{27}$ expressed as a function of $\hat{s}$ and the integration variable w. We obtain

$$\bar{\Delta} i_{23} = -2 + \frac{4}{w-\hat{s}} \left[z\, G_{-1}\Big(\frac{\hat{s}}{z}\Big) - z\, G_{-1}\Big(\frac{w}{z}\Big) - \frac{\hat{s}}{2}\, G_0\Big(\frac{\hat{s}}{z}\Big) + \frac{\hat{s}}{2}\, G_0\Big(\frac{w}{z}\Big) \right] , \tag{28}$$

$$\bar{\Delta} i_{27} = 2 \left[G_0\Big(\frac{\hat{s}}{z}\Big) - G_0\Big(\frac{w}{z}\Big) \right] , \tag{29}$$

where the functions $G_k(t)$ $(k \geq -1)$ are defined through the integral

$$G_k(t) = \int_0^1 dx\, x^k \, \ln\left[1 - t\, x(1-x) - i\,\delta\right] , \quad G_1(t) = \frac{1}{2} G_0(t).$$

Explicitly, the functions $G_{-1}(t)$ and $G_0(t)$ read

$$G_{-1}(t) = \begin{cases} 2\,\pi\,\arctan\Big(\sqrt{\frac{4-t}{t}}\Big) - \frac{\pi^2}{2} - 2\,\arctan^2\Big(\sqrt{\frac{4-t}{t}}\Big), & t < 4 \\ \\ -2\,i\,\pi\,\ln\Big(\frac{\sqrt{t}+\sqrt{t-4}}{2}\Big) - \frac{\pi^2}{2} + 2\,\ln^2\Big(\frac{\sqrt{t}+\sqrt{t-4}}{2}\Big), & t > 4 \end{cases}, \tag{30}$$

$$G_0(t) = \begin{cases} \pi\,\sqrt{\frac{4-t}{t}} - 2 - 2\,\sqrt{\frac{4-t}{t}}\,\arctan\Big(\sqrt{\frac{4-t}{t}}\Big), & t < 4 \\ \\ -i\,\pi\sqrt{\frac{t-4}{t}} - 2 + 2\,\sqrt{\frac{t-4}{t}}\,\ln\Big(\frac{\sqrt{t}+\sqrt{t-4}}{2}\Big), & t > 4 \end{cases}. \tag{31}$$

6 Numerical results

First, we investigate the numerical impact of the finite bremsstrahlung corrections [see Eqs. (13 and (22)] on the dilepton invariant mass spectrum. Following common practice, we consider the ratio

$$R_{\text{quark}}(\hat{s}) = \frac{1}{\Gamma(b \to X_c\,e\,\bar{\nu}_e)} \frac{d\Gamma(b \to s\,\ell^+\ell^-)}{d\hat{s}}\,, \tag{32}$$

in which the factor $m_{b,\text{pole}}^5$ drops out. The explicit expression for the semi-leptonic decay width $\Gamma(b \to X_c\,e\,\bar{\nu}_e)$ reads

$$\Gamma(b \to X_c\,e\,\bar{\nu}_e) = \frac{G_F^2\,m_{b,\text{pole}}^5}{192\,\pi^3}\,|V_{cb}|^2\,g\left(\frac{m_{c,\text{pole}}^2}{m_{b,\text{pole}}^2}\right)\,K\left(\frac{m_c^2}{m_b^2}\right)\,, \tag{33}$$

where $g(z) = 1 - 8\,z + 8\,z^3 - z^4 - 12\,z^2\,\ln(z)$ is the phase space factor, and

$$K(z) = 1 - \frac{2\,\alpha_s(m_b)}{3\,\pi}\,\frac{f(z)}{g(z)} \tag{34}$$

incorporates the next-to-leading QCD correction to the semi-leptonic decay [18]. The function $f(z)$ has been calculated analytically in Ref. [19]. It reads

$$\begin{aligned} f(z) = &- (1-z^2)\,\left(\frac{25}{4} - \frac{239}{3}\,z + \frac{25}{4}\,z^2\right) + z\,\ln(z)\left(20 + 90\,z - \frac{4}{3}\,z^2 + \frac{17}{3}\,z^3\right) \\ &+ z^2\,\ln^2(z)\,(36 + z^2) + (1-z^2)\,\left(\frac{17}{3} - \frac{64}{3}\,z + \frac{17}{3}\,z^2\right)\,\ln(1-z) \\ &- 4\,(1 + 30\,z^2 + z^4)\,\ln(z)\ln(1-z) - (1 + 16\,z^2 + z^4)\,\big(6\,\text{Li}(z) - \pi^2\big) \\ &- 32\,z^{3/2}(1+z)\left[\pi^2 - 4\,\text{Li}(\sqrt{z}) + 4\,\text{Li}(-\sqrt{z}) - 2\ln(z)\,\ln\left(\frac{1-\sqrt{z}}{1+\sqrt{z}}\right)\right]\,. \end{aligned} \tag{35}$$

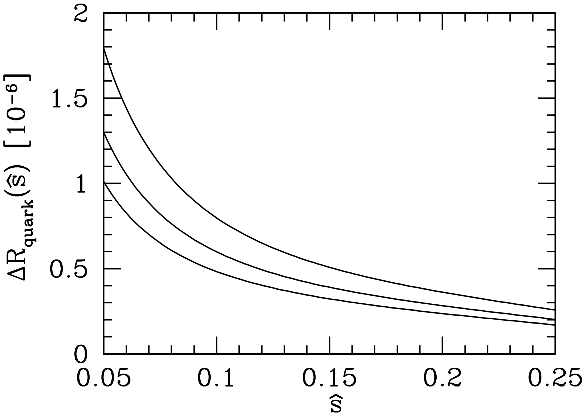

Figure 7: The new contribution $\Delta R_{\mathrm{quark}}(\hat{s})$ due to finite bremsstrahlung corrections for $\mu = 2.5$ GeV (uppermost curve), $\mu = 5$ GeV (middle curve) and $\mu = 10$ GeV (lowest curve) and $m_c/m_b = 0.29$.

We stress that the function $f(z)$ refers to on-shell renormalization of the charm quark mass.

In Fig. 7 we consider the contribution $\Delta R_{\mathrm{quark}}(\hat{s})$, which is due to the finite bremsstrahlung corrections in Eqs. (13) and (22), for three values of the renormalization scale (μ=2.5, 5 and 10 GeV) and for fixed value $m_c/m_b = 0.29$. The values of all the other input parameters are as in Ref. [1]. In Fig. 8 we combine the new corrections with the previous results. The solid lines show the ratio $R_{\mathrm{quark}}(\hat{s})$, including the new corrections, for the values $\mu = 10$ GeV (uppermost curve), $\mu = 5$ GeV (middle curve) and $\mu = 2.5$ GeV (lowest curve) and for fixed value $m_c/m_b = 0.29$. The dashed lines represent the corresponding results without the new corrections. We find that for $\hat{s} = 0.05$ the new corrections increase the ratio $R_{\mathrm{quark}}(\hat{s})$ by $\sim 3\%$, while for larger values of $\hat{s}$ their impact is even smaller. When including the finite bremsstrahlung corrections we obtain

$$R_{\mathrm{quark}} = \int\limits_{0.05}^{0.25} d\hat{s}\, R_{\mathrm{quark}}(\hat{s}) = (1.27 \pm 0.08(\mu)) \times 10^{-5}$$

for the integrated quantity R_{quark}. The error is obtained by varying μ between 2.5 GeV and 10 GeV. For comparison, the corresponding result without the finite bremsstrahlung correction is $R_{\mathrm{quark}}(\hat{s}) = (1.25 \pm 0.08(\mu)) \times 10^{-5}$ [1].

Among the errors on $R_{\mathrm{quark}}(\hat{s})$ due to uncertainties in the input parameters, the one related

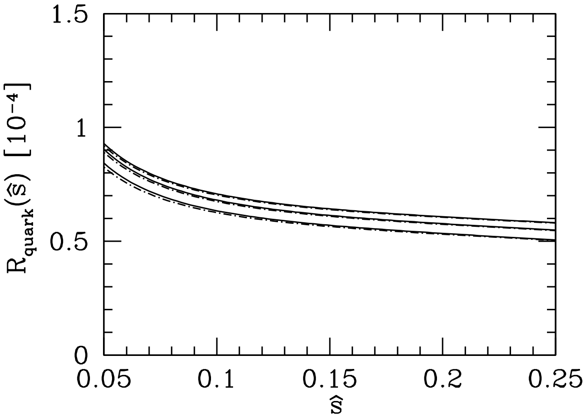

Figure 8: The solid curves show the ratio $R_{\text{quark}}(\hat{s})$ including the finite bremsstrahlung corrections while the dash-dotted curves show the corresponding results without the new corrections. The uppermost curves (solid and dash-dotted) correspond to $\mu = 10$ GeV, the middle curves to $\mu = 5$ GeV and the lowest curves to $\mu = 2.5$ GeV. $m_c/m_b = 0.29$.

to the charm quark mass is by far the largest. We therefore only comment on this error. In principle, the uncertainties induced by the charm quark mass have two sources. First, it is unclear whether m_c in the virtual- and bremsstrahlung corrections should be interpreted as the pole mass or the $\overline{\text{MS}}$ mass (at an appropriate scale). Second, the question arises what the numerical value of m_c is, once a choice concerning the definition of m_c has been made.

To illustrate these problems more clearly, it is useful to first consider the process $B \to X_s\gamma$. There, the one-loop matrix elements of O_1 and O_2 vanish, implying that the charm quark mass dependence only enters at $\mathcal{O}(\alpha_s)$. Formally, one can interpret m_c in these $\mathcal{O}(\alpha_s)$ expressions to be the pole mass or the $\overline{\text{MS}}$ mass because the difference is of higher order in α_s. Nevertheless, it has been argued in the literature [20] that the choice $m_c^{\overline{\text{MS}}}(\mu)$ with $\mu \in [m_c, m_b]$ seems more reasonable than m_c^{pole} (which was used in all the previous analysis) due to the fact that the largest charm quark mass dependence comes from the real part of the two-loop matrix elements of O_1 and O_2, where the charm quarks are usually off-shell, with a momentum scale set by m_b^{pole} (or some seizable fraction of it). It was shown in Ref. [20] that the definition of the charm quark mass leads to a relatively large uncertainty in the branching ratio: Changing m_c/m_b in $\Gamma(B \to X_s\gamma)$ from 0.29 ± 0.02 to 0.22 ± 0.04, i.e., from $m_c^{\text{pole}}/m_b^{\text{pole}}$ to $m_c^{\overline{\text{MS}}}/m_b^{\text{pole}}$ (with $\mu \in [m_c, m_b]$), causes an enhancement of $\text{BR}(B \to X_s\gamma)$ by $\sim 11\%$.

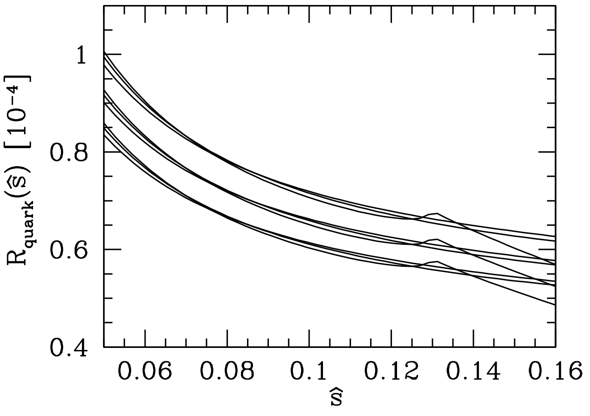

Figure 9: $R_{\text{quark}}(\hat{s})$ for various values and definitions of m_c: The three bands are obtained by setting $m_c^{\text{pole}}/m_b^{\text{pole}}$=0.31 (uppermost), 0.29 (middle) and 0.27 (lowest) in $\Gamma(b \to X_c\, e\, \bar{\nu}_e)$. In the rare decay $b \to X_s\, \ell^+\ell^-$ we set $m_c^{\overline{\text{MS}}}/m_b^{\text{pole}} = 0.18, 0.22, 0.26$. This leads to three curves all within a narrow band. See text.

In the process $B \to X_s\, \ell^+\ell^-$ this problem is less severe because m_c enters already the one-loop diagrams (i.e., at $\mathcal{O}(\alpha_s^0)$) associated with O_1 and O_2. As the two-loop calculation requires the renormalization of m_c, the definition of m_c has to be specified. Therefore, the two-loop result explicitly depends on the definition of the charm quark mass. This can be seen from [1]. For the pole mass definition, the results for the two-loop matrix elements of O_1 and O_2, encoded in $F_{1,2}^{(7),(9)}$, are given in Eqs. (54)–(56), while those corresponding to the $\overline{\text{MS}}$ definition are obtained by adding the terms $\Delta F_{1,2,m_c\text{ren}}^{\text{ct}(9)}$ given in Eq. (49).

In the following, we investigate the impact of pole- vs. $\overline{\text{MS}}$ definition of m_c in the rare decay $b \to X_s\, \ell^+\ell^-$ on the ratio $R_{\text{quark}}(\hat{s})$. In the semileptonic decay $b \to X_c\, e\, \bar{\nu}_e$ the charm quark is basically on-shell. Therefore, we always use the pole mass definition for the charm quark mass in $\Gamma(b \to X_c\, e\, \bar{\nu}_e)$, which enters $R_{\text{quark}}(\hat{s})$.

In Fig. 9 we set $m_c^{\text{pole}}/m_b^{\text{pole}}$ equal to 0.31, 0.29 and 0.27 in the decay width $\Gamma(b \to X_c\, e\, \bar{\nu}_e)$. In the rare decay $b \to X_s\, \ell^+\ell^-$, on the other hand, we use the $\overline{\text{MS}}$ definition for m_c, and put $m_c^{\overline{\text{MS}}}/m_b^{\text{pole}} = 0.18, 0.22$ and 0.26 (independently of $m_c^{\text{pole}}/m_b^{\text{pole}}$, to be on the conservative side). This leads, for a given value of $m_c^{\text{pole}}/m_b^{\text{pole}}$, to three curves which form a narrow band. The uppermost band corresponds to $m_c^{\text{pole}}/m_b^{\text{pole}} = 0.31$, the middle to 0.29 and the lowest to 0.27. The curves with the strange behavior for $\hat{s} > 0.13$ all belong to the lowest value $m_c^{\overline{\text{MS}}}/m_b^{\text{pole}} = 0.18$. As the result for the two-loop corrections was derived in

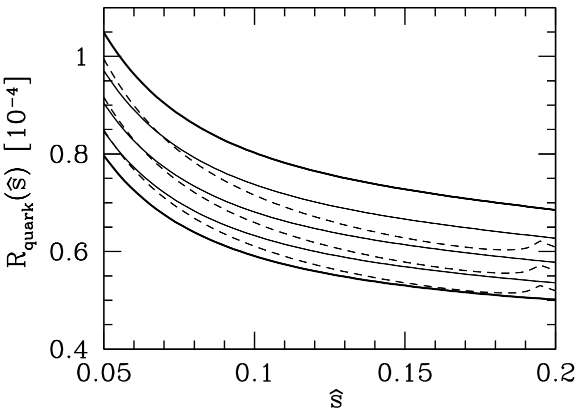

Figure 10: $R_{\mathrm{quark}}(\hat{s})$ for various values and definitions of m_c: The solid curves are obtained by setting $m_c^{\mathrm{pole}}/m_b^{\mathrm{pole}}$=0.33 (uppermost), 0.31, 0.29, 0.27 and 0.25 (lowest) in the rare- and the semileptonic decay. The dashed lines are obtained by taking $m_c^{\overline{\mathrm{MS}}}/m_b^{\mathrm{pole}} = 0.22$ in the rare decay and $m_c^{\mathrm{pole}}/m_b^{\mathrm{pole}}$= 0.31, 0.29 and 0.27 in $\Gamma(b \to X_c\, e\, \bar{\nu}_e)$. See text.

expanded form which only holds for $\hat{s} < 4\, m_c^2/m_b^2$, the strange behavior illustrates that, for $m_c/m_b = 0.18$, the result is not valid for $\hat{s} > 0.13$.

In Fig. 10 the three middle solid curves are obtained by adopting the pole mass definition of m_c, both in the rare and in the semileptonic decay. They correspond to $m_c^{\mathrm{pole}}/m_b^{\mathrm{pole}} = 0.31$, 0.29, 0.27. The dashed curves, on the other hand, are obtained when the $\overline{\mathrm{MS}}$ definition with $m_c^{\overline{\mathrm{MS}}}/m_b^{\mathrm{pole}} = 0.22$ is used in the rare decay width. One finds that for $\hat{s} > 0.06$ the results for $R_{\mathrm{quark}}(\hat{s})$ are somewhat larger when using the pole mass definition of m_c in the rare decay. For values below $\hat{s} < 0.06$ the situation is reversed and thus the same as for $b \to X_s \gamma$ [20]. Again, the strange behavior of the dashed curves indicates that, for $m_c/m_b = 0.22$, the expanded formulas become unreliable for values of $\hat{s} > 0.19$. The thick solid lines are obtained by adopting the pole mass definition on the whole and correspond to m_c/m_b=0.33 (upper) and 0.25 (lower). In summary, the figure shows that the quark mass uncertainties can effectively be estimated by working with the pole mass definition throughout, provided one takes the rather conservative range $0.25 \le m_c^{\mathrm{pole}}/m_b^{\mathrm{pole}} \le 0.33$.

Finally, in Fig. 11 we show $R_{\mathrm{quark}}(\hat{s})$ in the full range $\hat{s} \in [0.05, 0.25]$ for $m_c^{\mathrm{pole}}/m_b^{\mathrm{pole}} \in [0.25, 0.33]$. Note that for these values of m_c/m_b the expanded formulas hold just up to $\hat{s} = 0.25$.

Comparing Fig. 8 with Fig. 11, we find that the uncertainty due to m_c/m_b is clearly larger

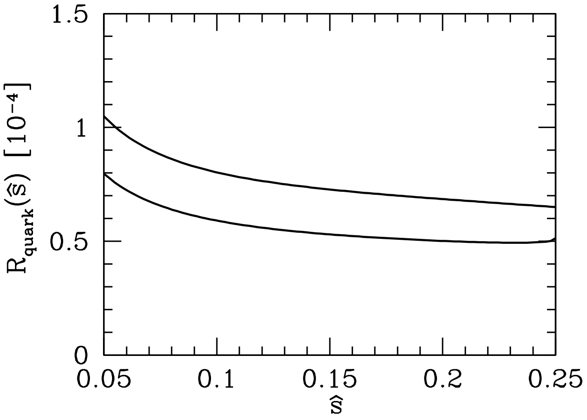

Figure 11: $R_{\text{quark}}(\hat{s})$ for $m_c^{\text{pole}}/m_b^{\text{pole}}$=0.33 (uppermost), 0.31, 0.29, 0.27 and 0.25 (lowest) in the rare- and the semileptonic decay in the full window $\hat{s} \in [0.05, 0.25]$.

than the leftover μ dependence. Varying m_c/m_b between 0.25 and 0.33, the corresponding uncertainty amounts to ±15%.

To conclude: We have calculated the finite gluon bremsstrahlung corrections of $\mathcal{O}(\alpha_s)$ to $\Gamma(b \to s\,\ell^+\ell^-)$, taking into account the contributions of the operators O_1, O_2, O_7, O_8, O_9 and O_{10}. We have worked out the numerical impact of the new corrections on the invariant mass spectrum of the lepton pair in the range $\hat{s} \in [0.05, 0.25]$ and found an increase of about 3% for $\hat{s} = 0.05$ and even less for larger values of $\hat{s}$. Furthermore, we investigated the uncertainties of $R_{\text{quark}}(\hat{s})$ due to the definition and numerical uncertainties of the charm quark mass. We found that these errors can be reliably estimated when working with the pole mass definition of m_c, provided one takes the rather conservative range $0.25 \leq m_c^{\text{pole}}/m_b^{\text{pole}} \leq 0.33$.

Acknowledgements:
The work of H.M.A. was partially supported by NATO Grant PST.CLG.978154.

A Auxiliary quantities A_i, T_9, U_9 and W_9

The auxiliary quantities A_i, T_9, U_9 and W_9, appearing in the modified Wilson coefficients in Eq. (3) and in the effective Wilson coefficients in Eqs. (7)–(9) are the following linear combinations of the Wilson coefficients $C_i(\mu)$ [16, 12]:

$$\begin{aligned}
A_7 &= \frac{4\,\pi}{\alpha_s(\mu)}\,C_7(\mu) - \frac{1}{3}\,C_3(\mu) - \frac{4}{9}\,C_4(\mu) - \frac{20}{3}\,C_5(\mu) - \frac{80}{9}\,C_6(\mu)\,,\\
A_8 &= \frac{4\,\pi}{\alpha_s(\mu)}\,C_8(\mu) + C_3(\mu) - \frac{1}{6}\,C_4(\mu) + 20\,C_5(\mu) - \frac{10}{3}\,C_6(\mu)\,,\\
A_9 &= \frac{4\pi}{\alpha_s(\mu)}\,C_9(\mu) + \sum_{i=1}^{6} C_i(\mu)\,\gamma_{i9}^{(0)}\,\ln\!\left(\frac{m_b}{\mu}\right) + \frac{4}{3}\,C_3(\mu) + \frac{64}{9}\,C_5(\mu) + \frac{64}{27}\,C_6(\mu)\,,\\
A_{10} &= \frac{4\pi}{\alpha_s(\mu)}\,C_{10}(\mu)\,, \qquad\qquad (36)\\
T_9 &= \frac{4}{3}\,C_1(\mu) + C_2(\mu) + 6\,C_3(\mu) + 60\,C_5(\mu)\,,\\
U_9 &= -\frac{7}{2}\,C_3(\mu) - \frac{2}{3}\,C_4(\mu) - 38\,C_5(\mu) - \frac{32}{3}\,C_6(\mu)\,,\\
W_9 &= -\frac{1}{2}\,C_3(\mu) - \frac{2}{3}\,C_4(\mu) - 8\,C_5(\mu) - \frac{32}{3}\,C_6(\mu)\,.
\end{aligned}$$

The elements $\gamma_{i9}^{(0)}$ can be found in [16], while the loop-function $h(z,\hat{s})$ is given in Eq. (4).

In the contributions which explicitly involve virtual or bremsstrahlung correction only the leading order coefficients $A_i^{(0)}$, $T_9^{(0)}$, $U_9^{(0)}$ and $W_9^{(0)}$ enter. They are given by

$$\begin{aligned}
A_7^{(0)} &= C_7^{(1)} - \frac{1}{3}\,C_3^{(0)} - \frac{4}{9}\,C_4^{(0)} - \frac{20}{3}\,C_5^{(0)} - \frac{80}{9}\,C_6^{(0)}\,,\\
A_8^{(0)} &= C_8^{(1)} + C_3^{(0)} - \frac{1}{6}\,C_4^{(0)} + 20\,C_5^{(0)} - \frac{10}{3}\,C_6^{(0)}\,,\\
A_9^{(0)} &= \frac{4\,\pi}{\alpha_s}\left(C_9^{(0)} + \frac{\alpha_s}{4\,\pi}\,C_9^{(1)}\right) + \sum_{i=1}^{6} C_i^{(0)}\,\gamma_{i9}^{(0)}\,\ln\!\left(\frac{m_b}{\mu}\right) + \frac{4}{3}\,C_3^{(0)} + \frac{64}{9}\,C_5^{(0)} + \frac{64}{27}\,C_6^{(0)}\,,\\
A_{10}^{(0)} &= C_{10}^{(1)}\,, \qquad\qquad (37)\\
T_9^{(0)} &= \frac{4}{3}\,C_1^{(0)} + C_2^{(0)} + 6\,C_3^{(0)} + 60\,C_5^{(0)}\,,\\
U_9^{(0)} &= -\frac{7}{2}\,C_3^{(0)} - \frac{2}{3}\,C_4^{(0)} - 38\,C_5^{(0)} - \frac{32}{3}\,C_6^{(0)}\,,\\
W_9^{(0)} &= -\frac{1}{2}\,C_3^{(0)} - \frac{2}{3}\,C_4^{(0)} - 8\,C_5^{(0)} - \frac{32}{3}\,C_6^{(0)}\,.
\end{aligned}$$

We list the leading and next-to-leading order contributions to the quantities A_i, T_9, U_9 and W_9 in Tab. 1.

μ	2.5 GeV	5 GeV	10 GeV
α_s	0.267	0.215	0.180
$C_1^{(0)}$	-0.697	-0.487	-0.326
$C_2^{(0)}$	1.046	1.024	1.011
$\left(A_7^{(0)},\ A_7^{(1)}\right)$	$(-0.360,\ 0.031)$	$(-0.321,\ 0.019)$	$(-0.287,\ 0.008)$
$A_8^{(0)}$	-0.164	-0.148	-0.134
$\left(A_9^{(0)},\ A_9^{(1)}\right)$	$(4.241,\ -0.170)$	$(4.129,\ 0.013)$	$(4.131,\ 0.155)$
$\left(T_9^{(0)},\ T_9^{(1)}\right)$	$(0.115,\ 0.278)$	$(0.374,\ 0.251)$	$(0.576,\ 0.231)$
$\left(U_9^{(0)},\ U_9^{(1)}\right)$	$(0.045,\ 0.023)$	$(0.032,\ 0.016)$	$(0.022,\ 0.011)$
$\left(W_9^{(0)},\ W_9^{(1)}\right)$	$(0.044,\ 0.016)$	$(0.032,\ 0.012)$	$(0.022,\ 0.009)$
$\left(A_{10}^{(0)},\ A_{10}^{(1)}\right)$	$(-4.372,\ 0.135)$	$(-4.372,\ 0.135)$	$(-4.372,\ 0.135)$

Table 1: Coefficients appearing Eqs. (7)–(9) for $\mu = 2.5$ GeV, $\mu = 5$ GeV and $\mu = 10$ GeV. For $\alpha_s(\mu)$ (in the $\overline{\text{MS}}$ scheme) we used the two-loop expression with five flavors and $\alpha_s(m_Z) = 0.119$. The entries correspond to the pole top quark mass $m_t = 174$ GeV. The superscript (0) refers to lowest order quantities.

References

[1] H. H. Asatryan, H. M. Asatrian, C. Greub and M. Walker, *Phys. Lett.* B **507**, 162 (2001), [hep-ph/0103087];
H. H. Asatryan, H. M. Asatrian, C. Greub and M. Walker, *Phys. Rev.* D **65**, 074004 (2002), [hep-ph/0109140].

[2] Z. Ligeti and M. B. Wise, *Phys. Rev.* D **53**, 4937 (1996).

[3] A. F. Falk, M. Luke and M. J. Savage, *Phys. Rev.* D **49**, 3367 (1994).

[4] A. Ali, G. Hiller, L. T. Handoko and T. Morozumi, *Phys. Rev.* D **55**, 4105 (1997).

[5] J-W. Chen, G. Rupak and M. J. Savage, *Phys. Lett.* B **410**, 285 (1997).

[6] G. Buchalla, G. Isidori and S. J. Rey, *Nucl. Phys.* B **511**, 594 (1998).

[7] G. Buchalla and G. Isidori, *Nucl. Phys.* B **525**, 333 (1998).

[8] F. Krüger and L.M. Sehgal, *Phys. Lett.* B **380**, 199 (1996).

[9] A. Ali, P. Ball, L.T. Handoko, G. Hiller, *Phys. Rev.* D **61**, 074024 (2000).

[10] E. Lunghi and I. Scimemi, *Nucl. Phys.* B **574**, 43 (2000).

[11] E. Lunghi, A. Masiero, I. Scimemi and L. Silvestrini, *Nucl. Phys.* B **568**, 120 (2000).

[12] A. Ali, E. Lunghi, C. Greub and G. Hiller, hep-ph/0112300.

[13] H. H. Asatryan, H. M. Asatrian, G. K. Yeghiyan and G. K. Savvidy, *Int. J. Mod. Phys.* **A16**, 3805 (2001).

[14] M. Misiak, *Nucl. Phys.* **B393** 23 (1993); E:**B439** 461 1995.

[15] A. J. Buras and M. Münz, *Phys. Rev.* D **52**, 186 (1995).

[16] C. Bobeth, M. Misiak and J. Urban, *Nucl. Phys.* B **574**, 291 (2000).

[17] K. Chetyrkin, M. Misiak and M. Münz, *Phys. Lett.* B **400**, 206 (1997).

[18] N. Cabibbo and L. Maiani, *Phys. Lett.* B **79**, 109 (1978).

[19] Y. Nir, *Phys. Lett.* B **221**, 184 (1989).

[20] P. Gambino and M. Misiak, *Nucl. Phys.* B **611**, 338 (2001), [hep-ph/0104034].